Iraqi Journal of Biotechnology, 2025, Vol. 24, No. 1, 173-186

Efficacy of Curcumin Selenium Nanoparticles to Target *GDF9* Gene and Redox Status in Doxorubicin Stressed Rats

[1]Rawya Sh. Mohammed, [2]Baraa N. Al-Okaily

[1,2] Department of Physiology, Biochemistry and Pharmacology, College of Veterinary Medicine, University of Baghdad

Received: March 7, 2024 / Accepted: March 28, 2024 / Published: March 5, 2025

Abstract: Background Curcumin extract contain many bioactive polyphenolic compound, such as curcuminoids, dimethoxy-curcumin and bisdemethoxycurcumin obtained from *curcuma longa* which exhibits a positive effect on female reproductive system**.**Current study was aimed to investigate the protective effect of synthesized curcumin selenium nanoparticles (CurSeNPs) utilizing hydroalcoholic extract derived from *Curcuma longa* (turmeric) in alleviating the disturbance of redox homeostasis and GDF9 gene expressions related to ovarian functions doxorubicin treated in female rats. CurSeNPs were synthesized by combining sodium selenite with an alcoholic extract of *Curcuma longa*, resulting in a color shift of the solution from light orange to orange-red after 24 hours. The UV spectroscopy data indicated absorption bands at a wavelength of 214 nm, FTIR analysis demonstrated that CurSeNPs compounds contain abundant OH, C-H, C=O, C=C, C-C, and amine groups. Additionally, X-RD analysis at 2 theta identified the formation type as curcumin and indicated the particle size to be within the range of 18–80 nm and EDX analysis has verified the existence of elemental selenium nanoparticles exhibited excellent stability, as evidenced by their high zeta potential. Besides, the FESEM picture demonstrated the existence of spherical CurSe nanoparticles within the size range of 21–37 nm, as confirmed by AFM. In vivo study, included thirty-two (32) adult female rats were randomly and evenly divided into four experimental groups and treated accordingly for a duration of two weeks as following: Control (C) group: Rats were administered orally distilled water, group G1: Rats were (IP) injection of Dox (4.40mg /kg B.W.), (G2) group: Rats were administered CurSeNPs (10.47 µg /kg B.W.) and (G3) group: Rats were subjected to both Doxorubicin and intubation with CurSeNPs at same doses. Blood samples were collected after 14 days of the experiment from anesthetized rats, then serum were obtained for measuring SOD and MDA. Furthermore, the specimens of ovaries tissues were extracted to analyze the gene expression of GDF9. The results pointed the creation of oxidative stress in the G1 group, characterized by a significant reduction in serum SOD concentration and GDF9 gene expression level associated with an increase in serum MDA levels. In contrast, the present trial showed that the administration of CurSeNPs in G2 and G3 groups has ability to the improvement the oxidative stress-related factors as well as increase the express of GDF9gene. It was concluded the current study demonstrated that CurSeNPs have both preventive and /or therapeutic effects against doxorubicin toxicity in adult female rats may be via as antioxidant and anticancer properties.

Keywords: Curcumin, Selenium nanoparticles, Doxorubicin, GDF9, MDA, SOD.

Corresponding Author: (Email: rawia.mirza2106p@covm.uobaghdad.edu.iq).

Introduction

Nanoparticles are tiny particles ranging in size from 1 to 100 nanometers, and they can have various shapes such as spherical, triangular, or rod-shaped. Present investigation focuses on synthesising nanoparticles because to their distinct observable properties (chemical, physical, optical) compared to bulk materials(1). Curcumin is one of several naturally occurring compounds (NPs) that include physiologically active chemicals with medicinal potential. One safe, efficient, low-cost, and non-toxic way to make selenium nanoparticles is by biosynthesis(2). These nanoparticles are more stable because they have a natural covering of organic molecules, and they do not accumulate with time (3). It was discovered that the bio-synthesized Fe2O3NPs exhibit potent antibacterial activity against the introduced microorganisms (4). The study showed that zinc sulphide nanoparticles (ZnS NPs) have antibacterial effects against Gram-positive bacteria (Staphylococcus aureus) found in antibiotic-resistant wounds (5). The production of stable silver nanoparticles (AgNPs) from olive leaves was a straightforward, cost-effective, and environmentally benign process (6). The black currant selenium nanoparticle acts as an antioxidant and hypolipidemic agent.It has both preventive and therapeutic effects in countering the toxic effects of D-galactose in adult male rats (7).

Silver nanoparticles can generate both pro and anti-inflammatory cytokines. They are considered harmless, non-toxic, and have strong anti-parasitic action. They can be utilized as an antileishmanial medication or as a supportive treatment for visceral leishmaniasis (8). The *Curcuma longa* plant is the source of the polyphenolic chemical known as curcumin. Its anti-inflammatory, anti-free radical, anti-cell, and anti-vascular properties are only a few of its numerous medicinal applications. The study found that nano-curcumin was synthesized using a straightforward and cost-effective method. The particles were confirmed to be nanoparticles, which have potential applications in many industries, medicine, and therapy(9). The importance of plant-based selenium nanoparticles (SeNPs) and the environmentally friendly methods used to synthesise them suggest that they will become a powerful therapeutic tool for treating deadly cancers and other serious medical conditions. Neurodegenerative illnesses, diabetes, viral infections, antibiotic and antifungal treatment resistance, and environmental applications are examples. Due to their potency, biocompatibility, and antibacterial characteristics, it’s may be useful in developing marketable antimicrobial drugs (10).

Doxorubicin is an extensively used anti-neoplastic drug used for solid and hematogenous cancer since the 1950s, and its usage is limited due to its toxic effects upon various organs. The main reason behind the toxicity is the production of free radicals. It is evident that the first and foremost organ affected by the doxorubicin is the heart, and further, it causes toxic effects in hepatic, kidney, reproductive organs, adipose tissue, and brain (11). Therefore, goal of this study is to examine the modern approaches to the synthesis and characterization of Cur-Se-NPs and study its protective role in alleviating the disturbance of redox homeostasis and gene expressions of GDF9 related to ovarian functions in female rats -induced by doxorubicin.

Materials and methods

Preparation and characterization of CurSeNPs

The rhizomes of *Curcuma longa* were acquired from the local market in Babel, Iraq. A *Curcuma longa* alcoholic extract was prepared according to the steps outlined in (12). After being carefully washed with distilled water, the 250 g of *Curcuma longa* rhizomes were dried in an incubator set at 40°C. After the rhizomes were dried, they were pulverised using a Sliver Crest blender. Using a magnetic hotplate stirrer, 50 grammes of *Curcuma longa* rhizomes and 500 milliliters of ethanol were mixed and stirred for six hours at a temperature of 70 to 80 °C. After that, at temperatures between 42 and 43 °C, the mixture was run through a rotary evaporator to extract the alcohol. Biological methods were used to create selenium nanoparticles using the aforementioned snippet. Mix 0.603g of sodium hydrogen selenite ($NaHSeO3$) with 100 ml of distilled water to make a solution with a molecular weight of 0.04 M. The mixture was subjected to sonication for 20 minutes and then stored in a dark place. In order to synthesize CurSeNPs (0.04M) from sodium selenite, the alcoholic extract of *Curcuma longa* was utilized as an efficient reducing agent. There was a 1:10 (volume/volume) ratio between the 1.8-gram extract and 50 milliliters of distilled water. The magnetic stirrer was used to agitate the liquid for three minutes at a temperature ranging from 40-45C. On a magnetic stirrer was placed 100 ml of the sodium selenite solution. Then, after stirring the mixture for four hours, 10 milliliters of the extract were added dropwise. The next day, the concoction was stored in a dark place. The color changes from a lighter orangish-red to a deeper orangish-red in the observation. A dark orange-red color was a telltale sign of CurSeNPs growth. After that, the sample was spun at 10,000 rpm for 20 minutes in a cooling centrifuge. Centrifuge the mixture at 6,000 rpm for 15 minutes to separate the solid particles from the clear liquid. Add 50 ml of distilled water. The procedure was iterated three times to eliminate organic impurities found in SeNPs and subsequently dried at a temperature of 45 ºC.

***In vivo* study of CurSeNPs**

The present investigation was done in the animal place related with the College of Veterinary Medicine at University of Baghdad. The present investigation employed on 32 adult female Wistar rats. Following the acclimation period, adult female rats were randomly and evenly divided into four experimental groups and treated accordingly for two weeks as following: Control (C) group: Rats were administered orally distilled water, group G1: Rats were intra-peritoneal (IP) injection of Doxorubicin at a dosage of 4.40mg /kg B.W. and group G2: Rats were administered CurSeNPs at a dosage of 10.47 µg /kg B.W. while group G3 were subjected to both an IP injection of Doxorubicin and intubation with CurSeNPs at the same doses. Blood samples were collected by cardiac puncture technique from anesthetized rats, then serum were obtained for measuring serum superoxide dismutase (SOD) and serum malondialdehyde (MDA) by using enzymatic kits (BTLAB .china) Animal care and treatment in this study was carried out at the College of Veterinary Medicine within the University of Baghdad in strict accordance with the code of ethics for animal experiments, and ethical approval was given through the local committee of animal care and use (P.G. 2641 date 29-11-2023).In addition, specimens ovarian tissues were taken out to assess the gene expression of GDF9. RNA extraction was performed using Genaid Korea's RNA extraction kit to obtain total RNA from the ovarian tissue. The quantification of gene expression was carried out using forward primer (5´-TTGCTGTTGCCTGTAGATGG-´3) and reverse primer (5´ -GAGCCGGACGGTATTGT-AGA-´3) (13) with the AddScript RT-qPCR Syber master kit from AddBio, Korea. The RT-qPCR results were evaluated based on the criteria outlined by Schmittgen and Livak (14). The values are provided as the means mean ± Standard deviation (SD), statistical analysis was conducted using one-way analysis of variance (ANOVA) and Least Significant Differences (LSD) test was used at a significant level of $P < 0.05$ to compare between groups, a computer program SPSS version 26 was used to analyze the data (15).

Results and discussion

(Figure 1) depicts the progressive alteration in color of the reaction mixture during the biosynthesis process. The creation of CurSeNPs was evidenced by the steady transition of the initial bright orange color to a darker orange-red hue after 40 minutes, indicating increased stability. The curcumin extract and sodium selenite react to affect the mixture's color. To create environmentally safe CurSeNPs, curcumin served as a reducing and stabilizing agent. Previous investigation have used a variety of green plants to generate the unique reddish-orange color of CurSeNPs nanoparticles (16). The color transition from yellow to reddish orange upon heating serves as an indication of an increase in particles size.

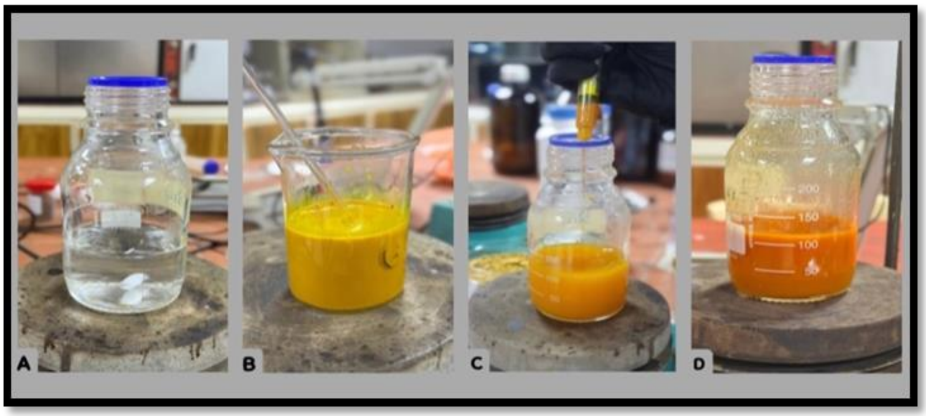

Figure (1): The image displayed the color transformation of sodium selenite into CurSeNPs by the use of an alcohol-based *Curcuma longa* extract. A: demonstrated a solution of sodium selenite lacking color; B: displayed an alcoholic extract of *Curcuma longa*; C: displayed curcumin selenium nanoparticles; and D: depicted an image of CurSeNPs after a 24-hour period.

UV- visible spectroscopy

UV-visible spectroscopy was used to analyse the colour changes of Cur-Se-NPs, *Curcuma longa*, and sodium selenite (Figure 1A-C). (Figure 2A) demonstrated that there was an impediment for the peak at 427 nm in the solution of *Curcuma longa*. In contrast, the solution of Cur-Se-NPs (Figure 2-C) exhibited a shift from 427 to 214 nm, indicating that curcumin, the primary constituent of turmeric (*Curcuma longa*), was present (17). The production of surface plasmon resonance (SPR) of selenium nanoparticles (Se NPs) is responsible for the UV-visible absorption peak observed at wavelengths spanning from

427 to 214 nm. However, a number of chemical synthesis techniques can produce commercial Se nanoparticles and green selenium nanoparticles have superior environmental benefits (18).

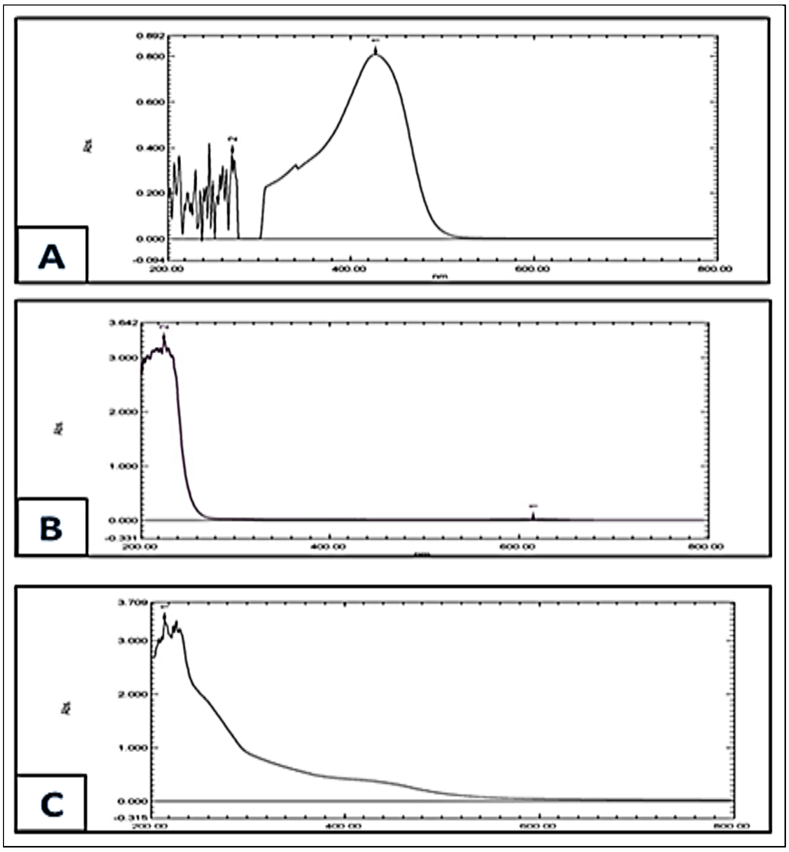

Figure (2): UV-Vis measure the absorbance of (A) :*Curcuma longa* extract (B): Sodium hydrogen selenite and (C): CurSeNPs.

Fourier transform infra-red (FTIR)

The FT-IR analysis of curcuma longa extract and synthesized Se NPs is shown in (Figure 3), with panels A, B representing the respective results. The FTIR spectroscopic examination of the alcoholic extract of *Curcuma longa* revealed distinct bands at different peaks ranging from 400 to 4000 cm1. This finding is consistent with (19). FT-IR studies were conducted to determine the functional groups and possible biomolecules that are involved in the capping and stabilization of SeNPs produced using *Curcuma longa* extract. The (Figures 3A, B) displayed distinct absorption bands in the FT-IR spectra of *Curcuma longa* extract and curSeNPs, respectively. The FT-IR spectra exhibited prominent absorption bands at (3755–3429 cm1) and indicating the presence of hydroxyl (-OH) or amine groups (-NH) (3402 cm1) in the *Curcuma longa* extract. This finding agrees with what Al-Ghareebawi found in the past; he also identified the absorption bands as belonging to a hydrophobic polyphenol that is used as a spice in cooking. The pharmaceutical business also makes extensive use of it (20). Alternatively, C-H stretch alkynes are indicated by the absorption peak at (2924, 2926 and 2854 cm−1). The plant extract included carbon dioxide

(0 = C = 0) as indicated by the peak at wavenumbers (2385 and 2370 cm−1). Around 1734, the absorption peaks. The carboxyl groups are represented by 06 cm-1. The C=C bond is associated with the absorption peaks at 1639 cm-1. The N-O bond is associated with the absorption peak at 1573 cm-1, whereas the C-H bond is represented by the peak at 1462.04 cm-1. Concerning the S = O, the absorption peaks may be seen around 1390.68 cm-1. The stretching of the C-N bonds in the amines is shown by the absorption peaks at 1269.16 cm-1 and 1163.80, 1124.50, 1116.78, 1068.56, 1041.56, 1037.56 cm-1. The stretching of C-X bonds in alkyl halides results in bands at 825.53, 840.96, and675.90 cm−1, whereas the bending of C-N-C bonds in amines generates the weak bands at 592.15 and 484.13 cm−1. Based on these results, it appears that there are a number of biomolecules with functional groups that might help stabilize and reduce the Se NPs. Previous research has provided more evidence that phytochemicals have a stabilizing role in the production of metal nanoparticles (21).

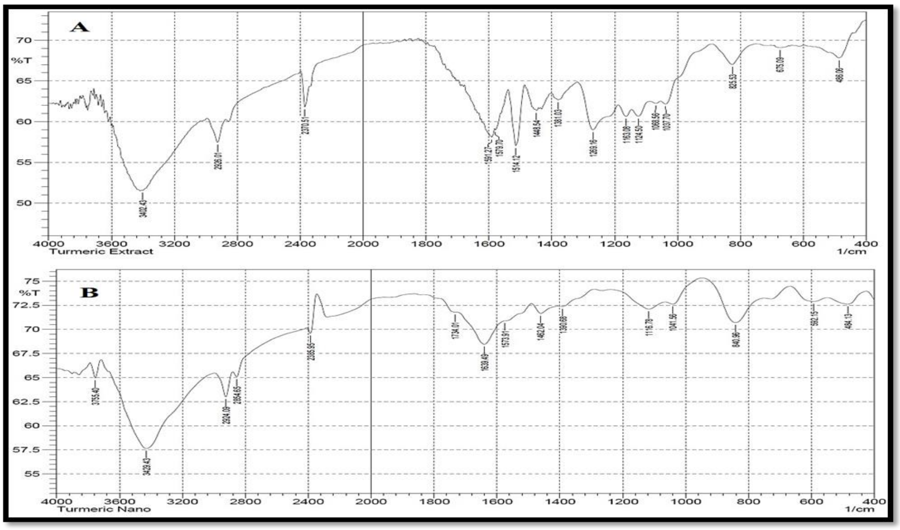

Figure (3 A): The FT-IR spectra of the alcoholic extract of *Curcuma longa* and (B) : the FT-IR spectrum of the functional groups of *Curcuma longa* extract coupled to SeNPs are provided.

X-Ray diffraction

The X-ray diffraction (XRD) test provides precise data on the size of nanomaterials and the crystal type present in a substance. The analytical XRD technique utilizes the angle theta-2 values of varied peaks (Figure 4) to determine the form and size of crystals. In this study, the Scherrer mathematical statement was used to analyze selenium nanoparticles produced by the alcoholic extraction of sodium selenite with *curcuma longa*. In the (100), (101), (110), (102), (111), (201) and (112) crystal planes, XRD peaks were seen at the theta angle-2 values of 20.446°, 26.990°, 28.042°, 29.677°, 48.73°, 51.683°, and 55.6465°, respectively, matching to the hkl values. The observed diffraction peaks are consistent with the standard card JCPDS No. 06-0362 and confirm the crystalline structure of curSe-NPs. Using the Scherrer equation for crystal planes, the data was analyzed. Also, results show that the produced chemical contains crystallized nanoparticles with a spherical form. Using the Debye-Scherrer equation, we were able to ascertain that the crystals had an average size ranging from 18 to 80 nm. (22).

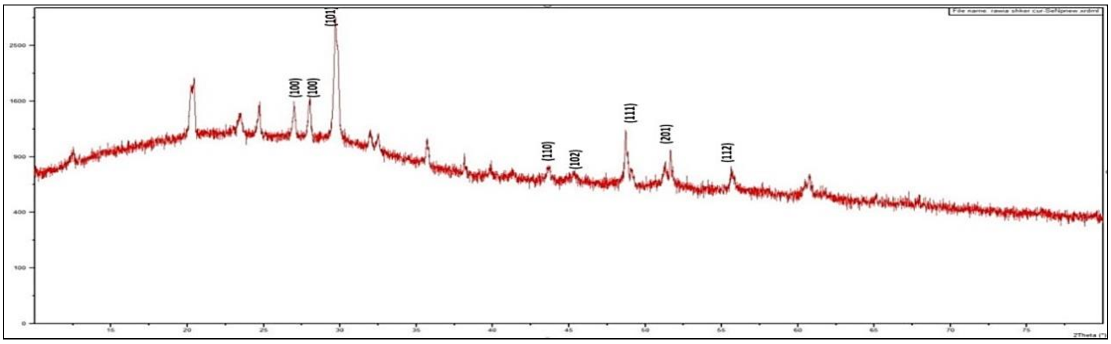

Figure (4): Sodium selenite solution and an alcoholic extract of *Curcuma longa* were used to synthesize curcumin selenium nanoparticles, which were characterized by the X-ray diffraction pattern

EDXS

The EDX analysis CurSe elemental composition of nanostructure's revealed a signal of C, O, and Na as shown in (Figure 5). These are likely caused by flavonoids and phenolics in the curcumin extract, which work as reducing agents. This indicates the existence of curcumin, which undergoes a nanotransformation when it reacts with selenium. These findings align with Shahbaz's report, which stated that SeNPs consist of selenium, oxygen, and carbon (23).

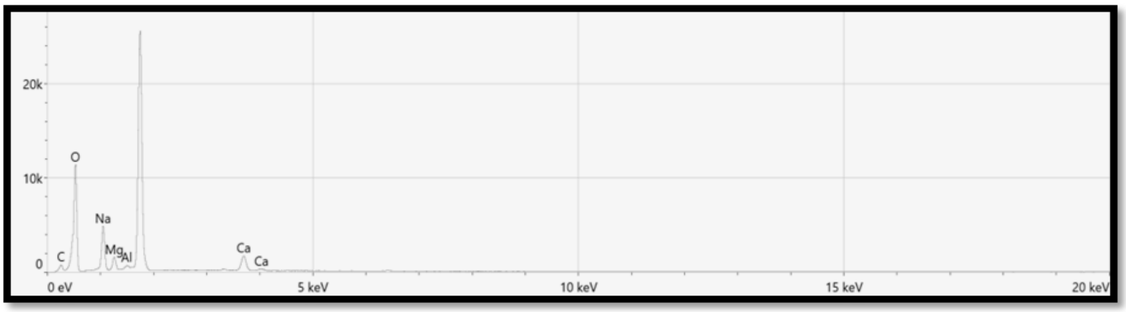

Figure (5): EDXS results for CurSe nanoparticles.

Zeta potential

In (Figure 6), the zeta potential's magnitude reveals information about the colloidal system's potential stability. According to zeta potential values, the stability degree is as follows: 0–10 mV indicates a state of high instability; 10–20 mV indicates a state of poor stability; 20–30 mV indicates a state of moderate stability; and values over 30 mV indicate a state of high stability. The zeta potential analysis of the Se-NPs synthesized in this work revealed a negative surface charge ranging from -120 to +60, with a specific value of -36.08 mV, as seen in Figure 6A. There is a negative value because of the polyphenolic and flavonoid parts of the reducing agent in the plant extract. These parts show electrostatic forces in the nanoparticles made from green materials (24). (Figure 6A) demonstrates that all particles in the synthesised solution possess a negative zeta potential value, which contributes to their high stability and prevents aggregation. Current results confirmed that the CurSeNPs were more stable because they were small and had a lower zeta potential. This made it easier for cells to absorb them and kept the integrity of their nanostructure.

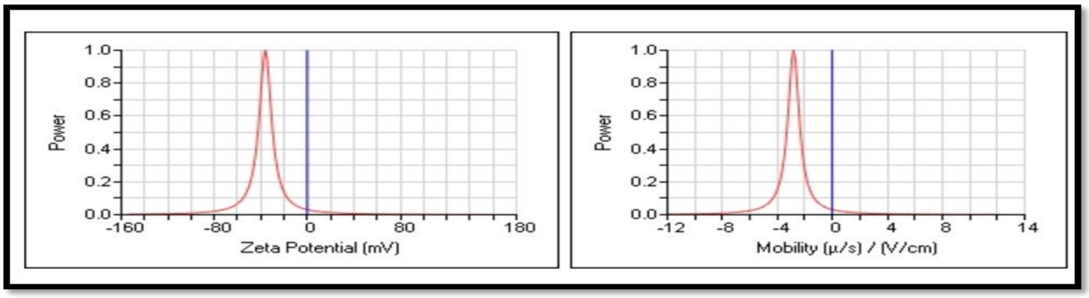

Figure (6): Zeta potentials of curcumin selenium nanoparticles A and B.

Field emission scanning electron micrographs (FE-SEM)

The goal of this test was to look at the shape and size of CurSeNPs, The FE-SEM pictures, seen at various magnifications, revealed the existence of spherical, amorphous structures with diameters ranging from 21 to 37 nm, as depicted in (Figure 7). The particles exhibited a uniform distribution with the occurrence of aggregation. Hence, it has been proposed that the aggregation of nanoparticles takes precedence over the reduction process and the initial formation of reduced atoms. In *Curcuma longa* extract, there are more functional groups that are better at binding and starting the formation of selenium acid ions, which may explain this. Furthermore, particles demonstrate two distinct regions: the illuminated outside sector and the shaded interior portion. Previous research on the production of selenium nanoparticles (SeNPs) has indicated that the findings of this study are supported by the presence of spherical Nanoparticles (21).

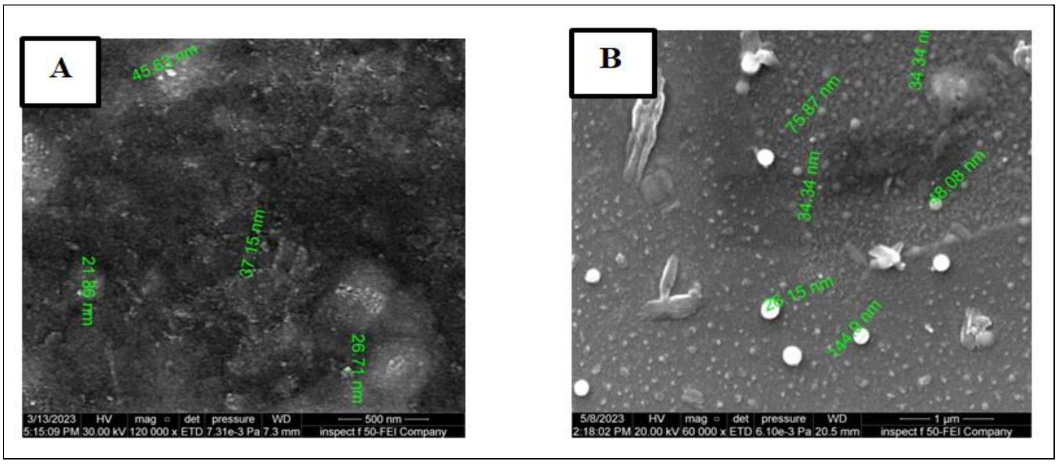

Figure (7): The FESEM image displayed the dimensions and properties of the synthesised Cur-Se-NPs, with (A) measuring 500nm and (B) measuring 1 µm.

Atomic force microscopy (AFM)

A surface's topography was examined using an atomic force microscope. Figure 8A displays a two-dimensional view of CurSeNPs, which appear as clusters of spherical shapes in either isolated or aggregated forms .While , the picture (8 B) displays a three-dimensional image of CurSeNPs, which exhibits a population of uniform particles with a smooth surface. In addition, (Figures 8C, D) demonstrated that the diameter of the synthesized curSeNPs varied between 3 and 43 nm, with a height of around 46.1n–48.1n. The acquired results have exhibited consistency with the data collected from the SEM analyses, while the outcomes of the AFM analysis have aligned with the findings reported in (25).

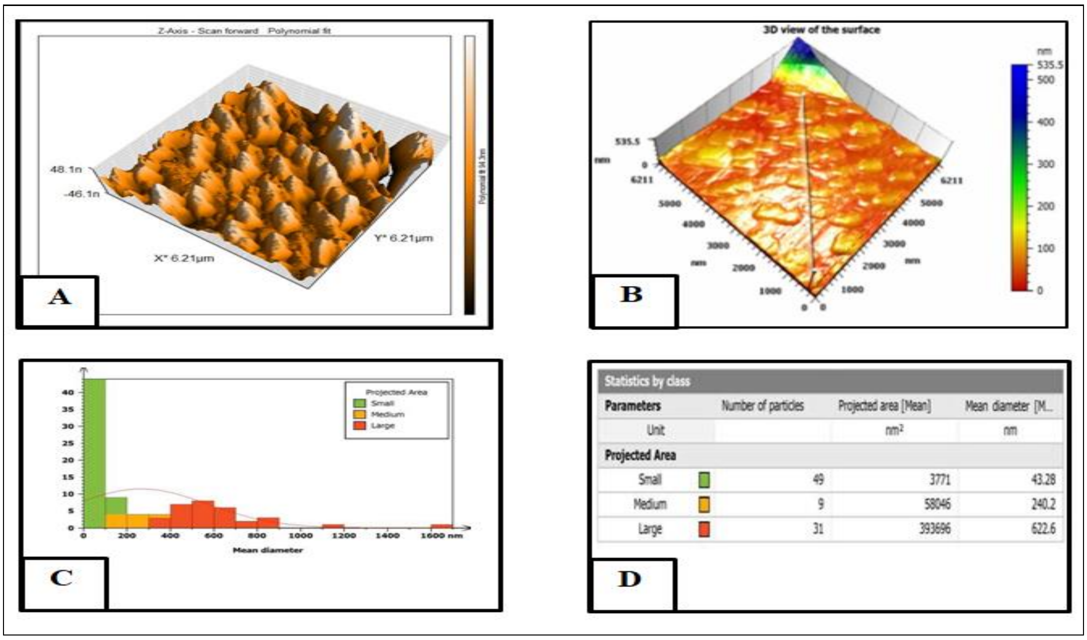

Figure (8): Atomic force microscopy (AFM) was used to analyze the size distribution of selenium nanoparticles (CurSeNPs). The results were shown in the form of a two-dimensional picture (a), a three-dimensional image (b), and a size distribution histogram (c) and (d)

Redox status

Doxorubicin treated group recorded significant (P < 0.05) decrease in compression with the other groups (table 1).While there was a significant (p < 0.05) reduction in serum MDA levels in groups G2 and G3, compared to group G1. In contrary, group G1 showed a significant (p<0.05) reduction in serum SOD concentration compared to the C, G2 and G3 groups. Besides, the findings showed significantly (p<0.05) elevated level of serum SOD in G2 and G3 treated groups (Table 1) compared to group (G1). This study found that doxorubicin caused oxidative stress in ovarian tissue via increasing lipid peroxidation (MDA) and decreasing SOD, indicating the potential for reproductive toxicity this similar with (26). The current findings reveal that the doxorubicin-treated group exhibited excessive synthesis of reactive oxygen species (ROS), leading to an elevation in malondialdehyde (MDA) levels in the ovary. These results may suggest a failure of the body to effectively eliminate ROS, possibly due to a decrease in the generation of antioxidants in response to the abundant production of free radicals. The ability of antioxidants to reduce the effects of chemotherapy has been underestimated during a period when it is becoming more crucial for finding techniques for preserving reproductive functions during chemotherapy (26, 27). The SOD plays an important role in the antioxidant defence system by protecting cells from oxidative damage through catalysis the conversion of superoxide radicals into less toxic compounds, such as hydrogen peroxide and molecular oxygen, via an enzymatic reaction The main function of Se is to protect cells from oxidation by the production of antioxidative mechanisms (28, 29). The SeNPs play a role in providing pharmacological protection against several inflammatory, oxidative stress and bacterial related diseases (30), may be attributed to their elevated nano-selenium content. As well as, nano-selenium content plays a crucial function in enhancing the activity of selenoenzymes, such as glutathione peroxidase. These selenoenzymes are important in safeguarding cells and tissues in vivo from the harmful effects of free radicals (31).

Table (1): Effect of CurSeNPs, doxorubicin and both on serum MDA and SOD in adult female rats after 14 days

Groups	Serum MDA	Serum SOD
Control	0.68 ± 0.10 c	1.62 ± 0.25 b
G1	1.45 ± 0.22 a	0.83 ± 0.09 c
G2	0.46 ± 0.12 c	2.93 ± 0.46 a
G3	0.99 ± 0.08 b	2.37 ± 0.87 a
LSD	0.19	0.68

Values are expresses as mean ± SD, n=5. C= Control group . G1 = Injected with i/p doxorubicin 4.40 mg /kg. b. w.G2 = Administrated with CurSeNPs 10.47 µg / kg bw. orally G3 = Administrated with CurSeNPs 10.47 µg / kg bw. orally and with doxorubicin 4.40 mg! kg b. w. i/p.Different small letters mean significantly differences between groups at P<0.05.

GDF9 genes expression in ovarian tissue

Current findings have been showed mRNA analysis of rats ovarian tissues revealed a significant decrease in the expression of the GDF9 gene in group G1 compared to the experimental groups. But, rats when received CurSeNPs with or without doxorubicin showed a significant ($P<0.05$) increase in expression of GDF9 compared to G1 group (table 2 and Figures 9 ,10) .A significant decrease of GDF9 gene expression in group G1 indicating a negative effects of doxorubicin on ovarian function . Two essential growth factors that play a role in regulating ovarian folliculogenesis are the interactions between oocyte and granulosa cells. The growth factors involved in this process are Growth Differentiation Factor 9 (GDF-9), which is produced by the oocyte and promotes the proliferation and differentiation of granulosa cells and stimulates oocyte maturation This results was agreement with (32). The GDF9 and BMP15 system regulates the growth, differentiation, and function of granulosa and thecal cells during follicular development through autocrine and paracrine mechanisms.

So, it plays a crucial role in oocyte development, ovulation, fertilization, and embryonic competence (33). In contrast serum levels of GDF-9 showing strong negative associations with age (34).SeNPs exhibited strong antioxidant effects in the ovaries, subsequently improved mitochondrial function, and provided significant anti-inflammatory effects by regulating inflammatory cytokines (35). Curcumin administration has been demonstrated to increase the expression of growth differentiation factor-9 (GDF-9) and bone morphogenetic protein 15 (BMP-15) and enhance the quantity of follicles in mouse ovaries (36). The anti-inflammatory effect of curcumin will enhance the interaction between oocytes and granulosa cells, leading to improved folliculogenesis through increased expressions of GDF-9 and KitL (37).

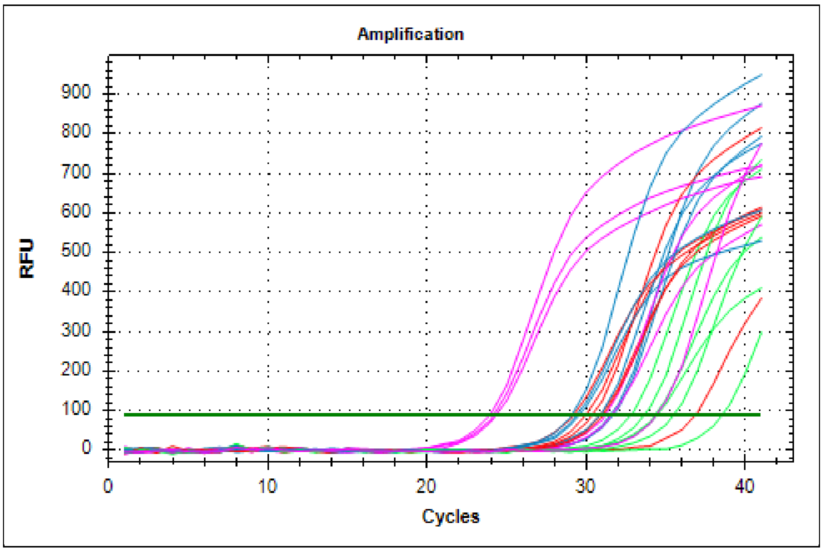

Figure (9): The real time amplification plots of *GDF9* gene expression of ovarian tissue in rats experimental samples. the real time PCR polts of *VEGF* gene. The blue plots (control group), green plots (G1 group), purple plots (G2group), red plots (G3 group).

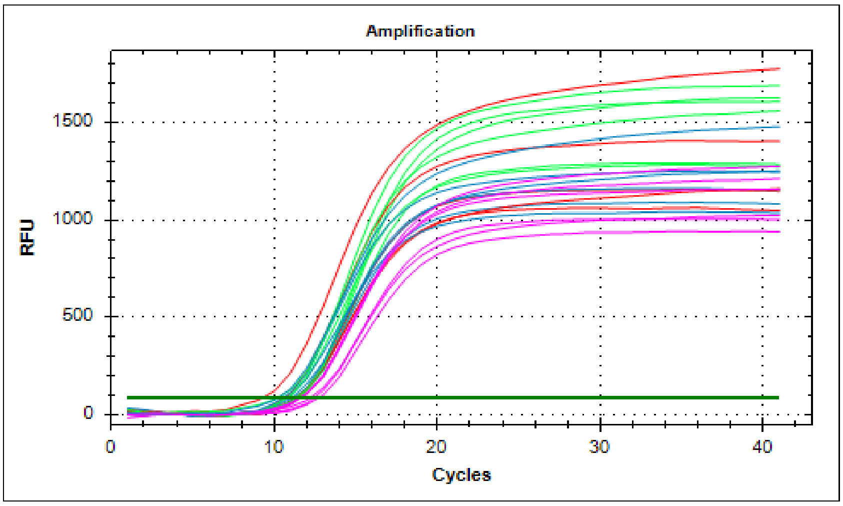

Figure (10): The real time amplification plots of house keeping (18S) gene expression of ovarian tissue in rats experimental samples. the real time PCR polts of PTEN gene. The blue plots (control group), green plots (G1 group), purple plots (G2group), red plots (G3 group).

Table (2): Effect of CurSeNPs, doxorubicin and both on GDF9 gene expression in adult female rats after 14 days

Groups	Fold change mRNA transcript level of PTEN gene
C	1.00 ± 0.00 b
G1	2.40 ± 1.03 a
G2	0.62 ± 0.39 b
G3	1.14 ± 0.38 b
LSD	0.70

Values are expresses as mean ± SD, n=5. C= Control group . G1 = Injected with i/p doxorubicin 4.40 mg /kg. b. w.G2 = Administrated with CurSeNPs 10.47 µg / kg bw. orally G3 = Administrated with CurSeNPs 10.47 µg / kg bw. orally and with doxorubicin 4.40 mg! kg b. w. i/p.Different small letters mean significantly differences between groups at $P<0.05$.

Conclusion

The biological synthesize of CurSeNPs using *Curcuma longa* extract to make nanoparticles naturally is an easy and inexpensive alternative to chemical synthesis that could be useful in biomedicine and it's have both preventive and / or therapeutic effects on ovarian doxorubicin toxicity in adult female rats. CurSeNPs can be regarded as antioxidant and anticancer therapy.

References

1. Al-Ahmer, S.D.; Shami, A.M. and AL-Saadi, B.Q.H. (2018). Using of Hybrid Nanoantibiotics as Promising Antimicrobial Agent. Iraqi Journal of Biotechnology, 17(3): 1-16
2. Ranjbar M.; Khakdan F. and Mukherjee A. (2023). In vitro analysis of green synthesized CuO nanoparticles using Tanacetum parthenium extract for multifunctional applications. Environmental Science and Pollution Research. 30(21): 60180–60195.
3. Alqayim, M.A. (2019). Biosynthesis, characterization and bioactivity of selenium nanoparticles synthesized by propolis. The Iraqi Journal of Veterinary Medicine.;43(1):197-209.
4. Yaaqoob, M.A. and Qasim, L.A. (2022). Effectivity of Iron Oxide Nanoparticles Synthesis by Intracellular *Lactobacillus* as Antibacterial Agent against *Pseudomonas aeruginosa*. Iraqi journal of biotechnology, 21(2): 428-438.
5. Ismail, B.A. and Zaidan, I. A. (2022). Effect of Biosynthesized ZnS Nanoparticles against Multi-Drug Resistance *Staphylococcus aureus* Isolated from Infected Wound. Iraqi Journal of Biotechnology, 21(2): 603-611
6. Salih, A.N.; Ibrahim, O.M. and Eesa, M.J. (2017). Antibacterial activity of biosynthesized sliver nanoparticles against Pseudomonas aeruginosa in vitro. The Iraqi Journal of Veterinary Medicine. 41(1): 60-65.
7. Khudair K. K.; Al-Kurdy, M.J. and Al-Kinani, L.H. (2020). Synthesis and Characterization of Black Currant Selenium Nanoparticles (Part I). The Iraqi Journal of Veterinary Medicine, 44 (2):25-34.
8. Mohamed, S.T.; Sulaiman, H.H.N.M.; Kamal, S.B. and Aja, H.A. (2019). Effect of Fusarium graminarum Silver-Nanoparticles on IL-10 and INF-γ Cytokines Levels in the Mice by Leishmania donovani in vivo. Iraqi Journal of Biotechnology, 18(2):106-115
9. Jaffar, H.I. and Hussein, S.I. (2015). Preparation and some characterization of curcumin-silica materials by sol-gel method. IJARSET. 6:1153-60
10. Ikram, M.; Javed, B.; Raja, N.I. and Mashwani, Z.U. (2021). Biomedical potential of plant-based selenium nanoparticles: a comprehensive review on therapeutic and mechanistic aspects. International Journal of Nanomedicine. Jan 12:249-268.

11. Renu, K.; Pureti, L.P. Vellingiri, B. and Valsala Gopalakrishnan, A. (2022). Toxic effects and molecular mechanism of doxorubicin on different organs–an update. Toxin Reviews. Apr 3;41(2):650-674.
12. Jayarambabu, N.; Akshaykranth, A.; Rao, T.V.; Rao, K.V.and Kumar, R.R. (2020). Green synthesis of Cu nanoparticles using Curcuma longa extract and their application in antimicrobial activity. Materials Letters. Jan 15; 259: 126813
13. Kobayashi, N.; Orisaka, M.; Cao, M.; Kotsuji, F.; Leader, A.; Sakuragi, N., *et al*. (2009). Growth differentiation factor-9 mediates follicle-stimulating hormone-thyroid hormone interaction in the regulation of rat preantral follicular development. Endocrinology, 150(12), 5566-5574.
14. Schmittgen, T.D. and Livak, K.J. (2008). Analyzing real-time PCR data by the comparative CT method. Nature protocols. Jun; 3(6): 1101-1108.
15. Baarda, B. and van Dijkum, C. (2019). Introduction to Statistics with SPSS. Routledge.
16. Sabea, A.M. and Al-Qaiym, M.A. (2023). Selenium synergize levothyroxine in restoring leukocytes cluster differentiation expression in methimazole induced hypothyroidism. Veterinary Science Journal - Veterinary & Animal Science; 11(10):1681-1689.
17. Soleimani, V.; Sahebkar, A. and Hosseinzadeh, H. (2018). Turmeric (Curcuma longa) and its major constituent (curcumin) as nontoxic and safe substances. Phytotherapy Research. Jun;32(6):985-995.
18. Ali, Z.S. and Khudair, K.K. (2019). Synthesis, characterization of silver nanoparticles using Nigella sativa seeds and study their effects on the serum lipid profile and DNA damage on the rats' blood treated with hydrogen peroxide. The Iraqi Journal of Veterinary Medicine; 43(2): 23-37.
19. Al-Musawi, A. T. (2022). Inhibitory activity of curcumin extract against some bacteria causing food poisoning isolated from some ready-to-eat meals. Caspian Journal of Environmental Sciences. Dec 1;20(5):1047-1052.
20. Al-Ghareebawi, A.M.; Al-Okaily, B.N. and Ibrahim, O.M. (2021). Characterization of Zinc Oxide Nanoparticles Synthesized by Olea Europaea Leaves Extract (Part L). Iraqi Journal of Agricultural Sciences. Jun 19;52(3): 580-588.
21. Al-Kurdy, M.J. and Khudair K. K. (2020). Effect of selenium loaded Ribes nigrum nanoparticles on genetic markers in male rats with D-galactose induced toxicity. (2020). OJVR, 24 (5): 312-327.
22. Fouda, A.; Hassan, S.E.; Eid, A.M.; Abdel-Rahman, M.A. and Hamza, M.F. (2022). Light enhanced the antimicrobial, anticancer, and catalytic activities of selenium nanoparticles fabricated by endophytic fungal strain, Penicillium crustosum EP-1. Scientific Reports. Jul 12; 12(1): 11834.
23. Shahbaz, M.; Akram, A.; Raja, N.I.; Mukhtar, T.; Mehak, A.; Fatima, N., *et al*. (2023). Antifungal activity of green synthesized selenium nanoparticles and their effect on physiological, biochemical, and antioxidant defense system of mango under mango malformation disease. PLoS One, 18(2): e0274679.
24. Nasrollahzadeh, M. and Sajadi, S.M. (2016). Green synthesis of Pd nanoparticles mediated by Euphorbia thymifolia L. leaf extract: catalytic activity for cyanation of aryl iodides under ligand-free conditions. Journal of colloid and interface science, 469: 191-195.
25. Kazemi, M.; Akbari, A.; Sabouri, Z.; Soleimanpour, S.; Zarrinfar, H.; Khatami, M., *et al*. (2021). Green synthesis of colloidal selenium nanoparticles in starch solutions and investigation of their photocatalytic, antimicrobial, and cytotoxicity effects. Bioprocess and Biosystems Engineering, 44: 1215–1225
26. Al-Okaily, B. N. and Murad, H. F. (2021). Role of alpha lipoic acid in protecting testes of adult rats from lead toxicity. Iraqi Journal of Veterinary Sciences, 35(2): 305-312.
27. Trujillo, M.; Odle, A. K., Aykin-Burns, N. and Allen, A. R. (2023). Chemotherapy induced oxidative stress in the ovary: drug-dependent mechanisms and potential interventions. Biology of Reproduction, 108(4): 522-537
28. Nwosu, N. C. and Onwuka, O. M. (2023). Cashew (Anarcadium occidentale) nut attenuates experimental model of nephrotoxicity induced by lead-mediated lipid peroxidation and impaired

histoarchitecture in kidney tissue. J Nutr Health Food Eng, 13(1): 6-9.

29. Al-Brakati, A.; Alsharif, K. F.; Alzahrani, K. J.; Kabrah, S.; Al-Amer, O.; Oyouni, A. A., *et al*. (2021). Using green biosynthesized lycopene-coated selenium nanoparticles to rescue renal damage in glycerol-induced acute kidney injury in rats. International Journal of Nanomedicine, 4335-4349.
30. Dawood, M. A.; Basuini, M. F. E.; Yilmaz, S.; Abdel-Latif, H. M.; Kari, Z. A.; Abdul Razab, M. K. A., *et al*. (2021). Selenium nanoparticles as a natural antioxidant and metabolic regulator in aquaculture: a review. Antioxidants, 10(9): 1364.
31. Bai, K.; Hong, B.; He, J. and Huang, W. (2020). Antioxidant capacity and hepatoprotective role of chitosan-stabilized selenium nanoparticles in concanavalin A-induced liver injury in mice. Nutrients, 12(3): 857.
32. Sanfins, A.; Rodrigues, P. and Albertini, D.F. (2018). GDF-9 and BMP-15 direct the follicle symphony. Journal of Assisted Reproduction and Genetics, 35: 1741-1750.
33. Aziz, A. Y. R.; Yu, X.; Jiang, Q.; Zhao, Y.; Deng, S.; Qin, K., *et al*. (2020). Doxorubicin-induced toxicity to 3D-cultured rat ovarian follicles on a microfluidic chip. Toxicology in Vitro, 62: 104677.
34. Gong, Y.; Li-Ling, J.; Xiong, D.; Wei, J.; Zhong, T. and Tan, H. (2021). Age-related decline in the expression of GDF9 and BMP15 genes in follicle fluid and granulosa cells derived from poor ovarian responders. Journal of Ovarian Research, 14: 1-10.
35. Jadaan, G.H. and Khudair, K.K. (2023). Curcumin phytosome as an anti-inflammatory and hypolipidemic in nano-silicon treated female rats. Veterinary Science Journal - Veterinary and Animal Science, 11(12): 2023-2029.
36. Azami, S. H.; Nazarian, H.; Abdollahifar, M. A.; Eini, F.; Farsani, M. A. and Novin, M. G. (2020). The antioxidant curcumin postpones ovarian aging in young and middle-aged mice. Reproduction, Fertility and Development, 32(3): 292-303.
37. Hendarto, H.; Widyanugraha, M.Y. and Widjiati, W. (2018). Curcumin improves growth factors expression of bovine cumulus-oocyte complexes cultured in peritoneal fluid of women with endometriosis. International Journal of Reproductive Biomedicine. Dec; 16 (12): 775-782.